American Journal of Engineering Research (AJER) 2020
American Journal of Engineering Research (AJER)
e-ISSN: 2320-0847 p-ISSN : 2320-0936
Volume-9, Issue-8, pp-186-193
www.ajer.org
Research Paper Open Access

A Comparative Study of Nonlinear Dynamics of a Quarter-Car Model Excited by Three Types of Humps/Bumps used in Ghana.

LawrenceAtepor
Department of Mechanical Engineering, Cape Coast Technical University, Box AD 50, Cape Coast, Ghana.

ABSTRACT: *This paper presents three types of humps/bumps commonly used in Ghana. They are Circular humps, speed bumps and trapezoidal humps. The vibrations of a quarter-car model are investigated theoretically across these humps/bumps to assess their effect on drivers and passengers. The study assumed elements of linear and nonlinear characteristics and the same height for all the humps/bumps. The velocity of the quarter-car is also assumed to be the same when crossing the profiles. The Method of Multiple Scales is used in solving the equations of motion and the steady-state solution is analyzed with the humps/bump inputs using the NDSolve* $Mathematica^{TM}$ *Software. Then comparing emanated amplitude results show that the trapezoidal hump has the smallest level of amplitude, thus more stable and lower vibration effect followed by the speed bump and the circular hump in that order.*

KEYWORDS: *Humps, Bumps, Vibration, Steady-state Solution, Amplitude*

Date of Submission: 15-08-2020 Date of acceptance: 01-09-2020

I. INTRODUCTION

It has always been quite stressful for passengers travelling on major and residential roads in Ghana as they endure the unpleasant experience of their vehicles struggling to climb dozens of speed humps, every now and then, on those roads. Speed humps have taken over the communities. Some of the humps are authorized but the illegal ones seem to outnumber those constructed legally. Speed humps are important traffic calming tools, which have helped to reduce accidents, especially those involving vehicles that knock down people in towns and villages. However, the rate at which they have been illegally constructed on the roads leaves much to be desired. Most of these speed humps cause nuisance to drivers and passengers and even pose a threat to lives of people, Arku [1] and with all attendant negative impacts like vibration on vehicles that use the road.

Akowuah et al [2], stated that speed humps are a major source of vibration hazard to vehicle occupants and that vibrations due to speed humps have grievous effects on pregnant women. Emslie [3] in his paper on Design and Implementation of Speed Humps: Supplementary to National Guidelines for Traffic Calming, stressed on the fact that speed humps are associated with noise production and vibrations emanating from acceleration and braking vehicles. Krylov [4] studied the ground-borne vibrations generated by road vehicles crossing road humps, and and speed cushions used for traffic calming. He generated analytical results and compared with existing experiments.

Dedovic [5] studied the effect of shock vibrations due to speed control humps to the health of city bus passengers using oscillatory model with six DOF and concluded that passenger's health, particularly of those using seats on rear platform, may be jeopardized even after one pass over the 5cm high rounded profile hump at 15km/h. They concluded that repeated and/or long-term exposure of human body to shock vibrations can produce musculoskeletal disorders and even injuries and that the influence of shock vibrations due to humps depends on the bus speed, geometry of the hump, the number of passes over and the passenger position in the bus.

Johnson and Nedzesky [6] compared speed humps, speed slots and speed cushions traffic reducing devices. Their study covered 12-22 ft. asphalt speed humps, 14 ft. prefabricated speed humps, 22 ft. speed slots and 10 ft. speed cushions. Weber [7] pointed out a number of hump designs including circular, trapezoidal, sinusoidal and combi. He quoted the dimensions of circular and sinusoidal humps. He used humps with 75-100 mm height and 3.7-9.1 m length. Berthod [8] stated that a sinusoidal shape is preferred over circular or parabolic shapes because it provides a more gentle transition. He quoted the dimensions of speed hump with and without flat centre. Hassan [9] presented a simple harmonic speed hump and studied the car dynamics during crossing

this hump using a quarter-car model. In Ghanathere are many types of speed humps in use but this study concentrates on the three most popular types, namely, the circular, trapezoidal and the round top speed bump.

The primary objective of this study is to compare the effect of these three different humps on the vehicle using vibration analysis and recommend the one that induces the lowest level of vibration for adoption in Ghana. To the best of the author's knowledge no one has used the method of vibration analysis to compare the different types of humps. A quarter-car model is usedfor the analysis.

The equations of motion were derived for a 2DOF Quarter-Car model excited by the humps. The Method of Multiple Scales (MMS) is used to solve the equations analytically to obtain the steady-state solution involving the excitation amplitudes, detuning parameter and the system's responses. Then Wolfram $Mathematica^{TM}$ is used to evaluate the steady-state solution for the three types of humps.

II. THE QUARTER-CAR MODEL

Most practical vibrating systems are very complex and it is almost impossible to consider all the details for mathematical analysis. Only the most important features are considered in the analysis to predict the behavior of the system under specific input conditions. A quarter-car with 2DOF is considered in this work. The analysis of the system involves derivation of the equations of motion, solution of the equations and interpretation of the results. The model of Fig. 1 consists of one tire and wheel and its attachments having the parameters: mass(m_2), damping coefficient (c_2) and stiffness (k_2). Where, m_1 is the primary mass (made up of the car seat and passenger), k_1 is the nonlinear suspension stiffness and c_1 is the damper coefficient of the primary mass.

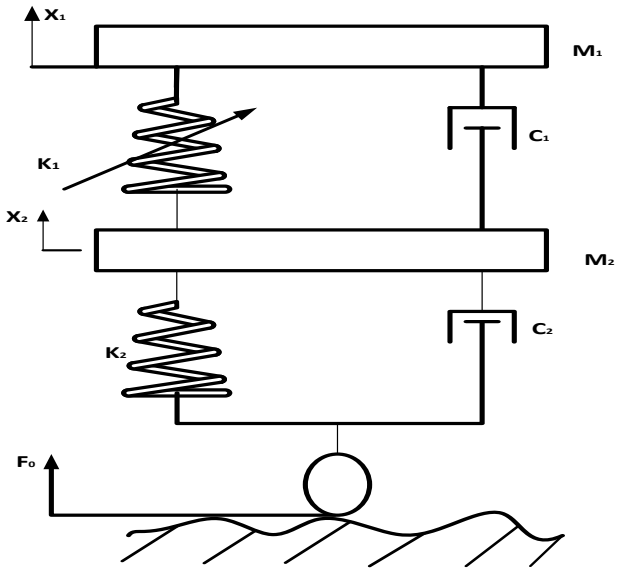

Fig. 1. Quarter-Car Model

The Nonlinear equations of motion are given by:

$$m_1\ddot{x}_1 + k_1(x_1 - x_2)^3 - c_1(\dot{x}_1 - \dot{x}_2) = 0 \quad (1)$$

$$m_2\ddot{x}_2 + k_2x_2 + c_2\dot{x_2} - k_1(x_1 - x_2)^3 - c_1(\dot{x}_1 - \dot{x}_2) = F_0x_2 (2)$$

Where, F_0 is the effect of the hump on the system and is a sinusoidal input motion given as,

$F_0 = Y \sin\left(\Omega t\right)(3)$

Where, Ω is the excitation frequency and Y is the amplitude of the road hump/bump.The angular frequency Ω is related to the displacement wave period τ through,

$$\Omega = 2\pi/\tau = \pi/T \quad (4)$$

Where, τ is twice the interval T. the time T is related to the car speed V (Km/h) through,

$$T = L/(1000V/3600) = 3.6L/V \text{ s}(5)$$

Where, L is the length of the hump concern. Combining equations (4) and (5) gives,

$$\Omega = \pi V/3.6L \text{ rads/s}(6)$$

III. HUMP/BUMP MODELING

In order to analyze the effect of a hump/bump on a vehicle and passengers we must model the hump/bump geometry. The hump/bump geometry is based on two basic inputs: the height (H) and the length (L) as depicted in Fig. 2.

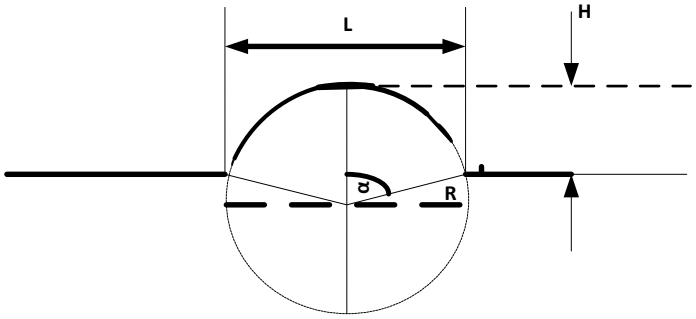

Fig. 2. Hump Modeling (Garcia-Pozuela et al [10])

Attending to hump/bump regulations, the hump/bump must be part of a circle. Unified height are used in the present research for the three types of humps/bumps.

3.1 Circular Hump

The circular hump has the dimensions: Height (H) and Length (L). A circular hump is simply a cylinder sector.

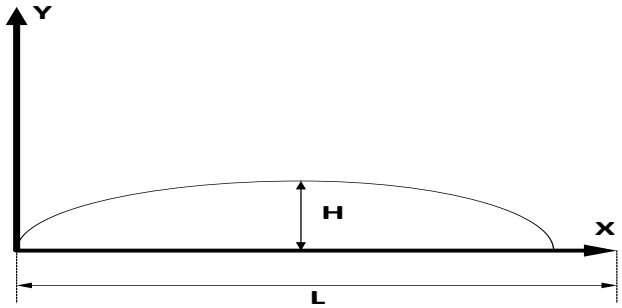

Fig. 3. Circular Hump

In the x-yplaneit has the mathematical model taken form Hassan [9] as

$$Y = \sqrt{\left\{R^2 - \left(0.5L - x\right)^2\right\}} - R\cos\alpha \quad \textbf{(7)}$$

Where, R is the hump/bump radius; L is the hump/bump length; α is the hump/bump sector angle between terminal radii; Y is the forcing amplitude and x-y are the coordinates of any point on the hump/bump from the hump/bump starting.

From Fig. 1 $R\sin\alpha = \frac{L}{2} \Rightarrow R = \frac{L}{2\sin\alpha}$ **(8)**

Also, $$H = R - R\cos\alpha \Rightarrow R = \frac{H}{1-\cos\alpha} \quad \textbf{(9)}$$

Equating (8) and (9) gives $$\frac{H}{1-\cos\alpha} = \frac{L}{2\sin\alpha} \quad \textbf{(10)}$$

Implying $$\frac{H\sin\alpha}{1-\cos\alpha} = \frac{L}{2} \quad \textbf{(11)}$$

Also, $$\sin\alpha = \sqrt{1-\cos^2\alpha} \quad \textbf{(12)}$$

Substituting (12) into (11) gives,

$$\frac{H\sqrt{1-\cos^2\alpha}}{1-\cos\alpha} = \frac{L}{2} \Rightarrow H\sqrt{1-\cos^2\alpha} = \frac{L}{2} - \frac{L}{2}\cos\alpha \quad \textbf{(13)}$$

Squaring (13) and rearranging gives

$$\left(\frac{L^2}{4}+H^2\right)\cos^2\alpha-\frac{L^2}{2}\cos\alpha+\left(\frac{L^2}{4}-H^2\right)=0 \textbf{ (14)}$$

Which can be written as

$$\left(\frac{L^2}{4}+H^2\right)z^2-\frac{L^2}{2}z+\left(\frac{L^2}{4}-H^2\right)=0 \textbf{ (15)}$$

Where, $z=\cos\alpha$

For a given Height (H) and Length (L), angle α used to define the hump/bump geometry is obtained by solving equation (15). Once angle α is found, the radius of the hump/bumpcircle is calculated either in terms of the height (H) or in Length (L) by using equations (8) or (9) and then Y is calculated.

3.2 Speed Bump

The speed bump is also circular in shape but shorter in Length. Model equation (7) can also be applied to the speed bump and its Y can be found by using equation (7).

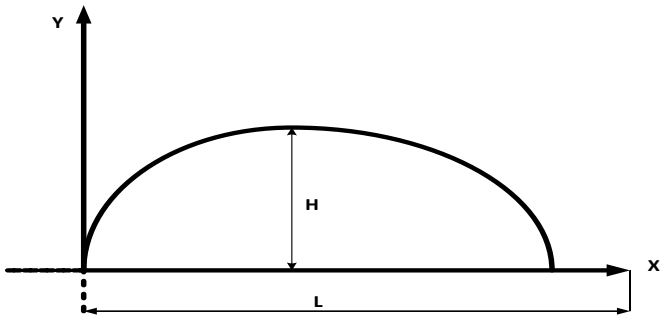

Fig. 3. Speed Bump

3.3 Trapezoidal Hump

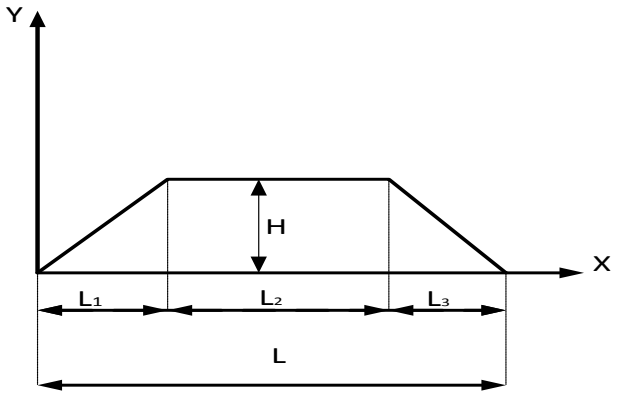

Figure 4: Trapezoidal Hump

The equations of the profile vertical deflection against the horizontal distance x is as given byHassan [9]

for $0\le x\le l_1; Y=0.5x$ **(16)**

for $l_1\le x\le l_1+l_2; Y=H$ **(17)**

for $l_1+l_2\le x\le L; Y=0.5x+\frac{L}{2}$ **(18)**

IV. SOLUTIONS TO THE EQUATIONS OF MOTION

The steady-state solution to the equations (1) and (2) are obtained for the system using the Method of Multiple Scales (MMS) as

$$\bar{\sigma}=2+\frac{\hat{c}_2^2\Omega}{2\omega_n^2}+\frac{\hat{c}_2\hat{c}_3\Omega}{2\omega_n^2}\pm\frac{4}{Y}\sqrt{\left(\eta_1+\eta_4\right)^2+\left(\eta_2+\eta_3\right)^2} \textbf{ (19)}$$

Where, $\bar{\sigma}$ is a detuning parameter and is a measure of the nearness to resonance, for the nondimensionalised case by means of $\frac{\Omega}{\omega_n} = \frac{\omega_n + \varepsilon\sigma}{\omega_n} = 1 + \frac{\varepsilon\sigma}{\omega_n} = 1 + \varepsilon\bar{\sigma}$ **(20)**

ω_n is the natural frequency of the system; $\hat{c}_2 = \frac{c_2}{m_2}$; $\hat{c}_3 = \frac{c_1}{m_2}$; $\hat{c}_1 = \frac{c_1}{m_1}$; ε is a small parameter introduced to order the equations (1) and (2) when nondimensionalising the time scale t. Where,

$$\eta_1 = \left\{ \begin{array}{l} -\frac{\hat{c}_1}{2\omega_n} p - \frac{\hat{c}_1}{2\omega_n} r + \frac{\hat{c}_1^2}{8\omega_n^2} q + \frac{\hat{c}_1^2}{8\omega_n^2} s - \frac{\hat{c}_1\hat{c}_2}{8\omega_n^2} s + \frac{\hat{c}_1\hat{c}_3}{8\omega_n^2} q - \frac{\hat{c}_1\hat{c}_3}{8\omega_n^2} s \\ + \frac{3\omega_1}{2\omega_n^2} p^2 q + \frac{3\omega_1}{2\omega_n^2} q^3 + \frac{3\omega_1}{\omega_n^2} p^2 s + \frac{3\omega_1}{\omega_n^2} q^2 s - \frac{3\omega_1}{\omega_n^2} pqr + \frac{3\omega_1}{2\omega_n^2} p^2 s \\ - \frac{3\omega_1}{\omega_n^2} q^2 s + \frac{3\omega_1}{\omega_n^2} qr^2 + \frac{3\omega_1}{\omega_n^2} qs^2 + \frac{3\omega_1}{\omega_n^2} prs - \frac{3\omega_1}{2\omega_n^2} qr^2 + \frac{3\omega_1}{2\omega_n^2} qs^2 \\ + \frac{3\omega_1}{2\omega_n^2} r^2 s + \frac{3\omega_1}{2\omega_n^2} s^3 \end{array} \right\} \quad \textbf{(21)}$$

$$\eta_2 = \left\{ \begin{array}{l} -\frac{\hat{c}_1}{2\omega_n} q - \frac{\hat{c}_1}{2\omega_n} s - \frac{\hat{c}_1^2}{8\omega_n^2} p - \frac{\hat{c}_1^2}{8\omega_n^2} r + \frac{\hat{c}_1\hat{c}_2}{8\omega_n^2} r - \frac{\hat{c}_1\hat{c}_3}{8\omega_n^2} p + \frac{\hat{c}_1\hat{c}_3}{8\omega_n^2} r \\ - \frac{3\omega_1}{2\omega_n^2} p^3 - \frac{3\omega_1}{2\omega_n^2} pq^2 - \frac{3\omega_1}{\omega_n^2} p^2 r - \frac{3\omega_1}{\omega_n^2} q^2 r + \frac{3\omega_1}{2\omega_n^2} p^2 r - \frac{3\omega_1}{2\omega_n^2} q^2 r \\ + \frac{3\omega_1}{\omega_n^2} pqs - \frac{3\omega_1}{\omega_n^2} pr^2 - \frac{3\omega_1}{\omega_n^2} ps^2 - \frac{3\omega_1}{2\omega_n^2} pr^2 + \frac{3\omega_1}{2\omega_n^2} ps^2 - \frac{3\omega_1}{\omega_n^2} qrs \\ - \frac{3\omega_1}{2\omega_n^2} r^3 - \frac{3\omega_1}{2\omega_n^2} rs^2 \end{array} \right\} \quad \textbf{(22)}$$

$$\eta_3 = \left\{ \begin{array}{l} -\frac{\hat{c}_2}{2\omega_n} r + \frac{\hat{c}_3}{2\omega_n} p - \frac{\hat{c}_3}{2\omega_n} r - \frac{\hat{c}_2^2}{8\omega_n^2} s + \frac{\hat{c}_2\hat{c}_3}{8\omega_n^2} q - \frac{\hat{c}_2\hat{c}_3}{4\omega_n^2} s - \frac{\hat{c}_1\hat{c}_3}{8\omega_n^2} q + \frac{\hat{c}_1\hat{c}_3}{8\omega_n^2} s \\ + \frac{\hat{c}_3^2}{8\omega_n^2} q - \frac{\hat{c}_3^2}{8\omega_n^2} s - \frac{3\omega_2}{2\omega_n^2} p^2 q - \frac{3\omega_2}{2\omega_n^2} q^3 + \frac{3\omega_2}{\omega_n^2} p^2 s + \frac{3\omega_2}{\omega_n^2} q^2 s + \frac{3\omega_2}{\omega_n^2} pqr + \frac{3\omega_2}{2\omega_n^2} p^2 s \\ - \frac{3\omega_2}{2\omega_n^2} q^2 s - \frac{3\omega_2}{\omega_n^2} qr^2 - \frac{3\omega_2}{\omega_n^2} qs^2 - \frac{3\omega_2}{\omega_n^2} prs + \frac{3\omega_2}{2\omega_n^2} qr^2 - \frac{3\omega_2}{2\omega_n^2} qs^2 - \frac{3\omega_2}{2\omega_n^2} r^2 s \\ - \frac{3\omega_2}{2\omega_n^2} s^3 \end{array} \right\} \quad \textbf{(23)}$$

$$\eta_4 = \left\{ \begin{array}{l} -\frac{\hat{c}_2}{2\omega_n} s + \frac{\hat{c}_3}{2\omega_n} q - \frac{\hat{c}_3}{2\omega_n} s + \frac{\hat{c}_2^2}{8\omega_n^2} r - \frac{\hat{c}_2\hat{c}_3}{8\omega_n^2} p + \frac{\hat{c}_2\hat{c}_3}{4\omega_n^2} r + \frac{\hat{c}_1\hat{c}_3}{8\omega_n^2} p - \frac{\hat{c}_1\hat{c}_3}{8\omega_n^2} r \\ -\frac{\hat{c}_3^2}{8\omega_n^2} p + \frac{\hat{c}_3^2}{8\omega_n^2} r + \frac{3\omega_2}{2\omega_n^2} p^3 + \frac{3\omega_2}{2\omega_n^2} pq^2 - \frac{3\omega_2}{\omega_n^2} p^2 r - \frac{3\omega_2}{\omega_n^2} q^2 r - \frac{3\omega_2}{2\omega_n^2} p^2 r + \frac{3\omega_2}{2\omega_n^2} q^2 r \\ +\frac{3\omega_2}{\omega_n^2} pqs + \frac{3\omega_2}{\omega_n^2} pr^2 + \frac{3\omega_2}{\omega_n^2} ps^2 + \frac{3\omega_2}{2\omega_n^2} pr^2 - \frac{3\omega_2}{2\omega_n^2} ps^2 + \frac{3\omega_2}{\omega_n^2} qrs + \frac{3\omega_2}{2\omega_n^2} r^3 \\ +\frac{3\omega_2}{2\omega_n^2} rs^2 \end{array} \right\} \quad (24)$$

Where, $\omega_1 = \frac{k_1}{m_1}$; $\omega_2 = \frac{k_1}{m_2}$; $\omega_n = \sqrt{\frac{k_2}{m_2}}$; p, q, r and s are steady-state amplitudes whose values are obtained by solving equations (21) to (24) simultaneously using *Mathematica*™ code.

V. RESULTS AND ANALYSIS

The parameters of the quarter-car model are given in Table 1, those of the humps and bump in Table 2 and the amplitudes in Table 3.

Table 1. Quarter-Car Model Parameters (Salem [11]).

Parameters	Description	Value
k_1 (kN/m^3)	Nonlinear Suspension stiffness	17.7
c_1 (kNs/m)	Suspension Damping Coefficient	37.5
m_1 (kg)	Car Body Mass	117
k_2 (kN/m)	Tire Stiffness	120
c_2 (kNs/m)	Tire Damping Coefficient	1.4
m_2 (kg)	Wheel Mass	36

Table 2. Humps/Bump Parameters

Parameters	Circular Hump	Speed Bump	Trapezoidal Hump
Height (H) m	0.1	0.1	0.1
Length (L) m	2	0.6	2.5
Forcing Amplitude Y m	4.47	1.79	1.72
Excitation Frequency Ω rad/s	24.2	80.7	19.4

Table 3. Amplitude Values

Parameters	Value
p	0.001
q	0.00025
r	0.0003
s	0.002

5.1 Amplitude of Response Plots

Four algebraic solutions for the amplitudes and phases, equations (21) to (24) were derived , which led to the steady-state solution of equation (19) describing the relationship between excitation amplitude, Y, detuning parameter, σ , and the system's responses. To obtain the values for p, q, r and s *Mathematica*™ code was used to solve the equations (21) to (24) simultaneously. The results obtained are in the time domain and are transformed into the frequency domain by running the *Mathematica*™ code several times for a range of frequency values from 52.1rad/s to 61.7 rad/s to obtain a list of amplitude values.

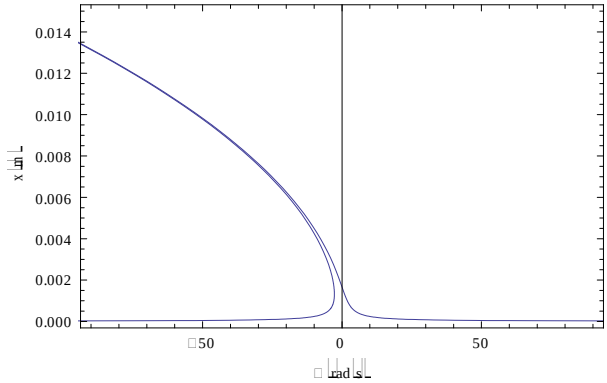

Fig. 4.Amplitude of response as a function of detuning frequency for Circular Hump

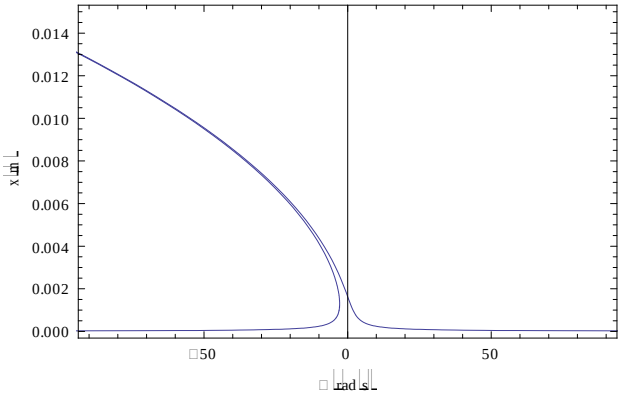

Fig. 5.Amplitude of response as a function of detuning frequency for Speed Bump

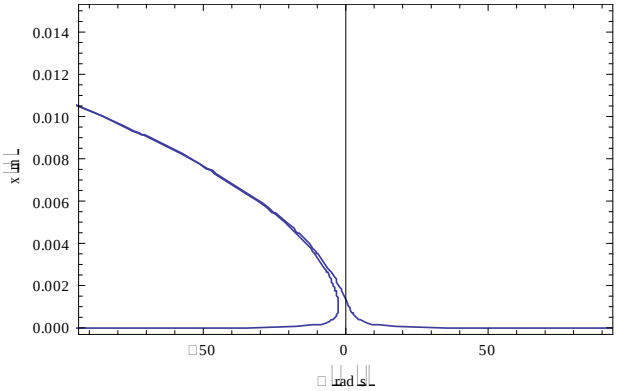

Fig. 6.Amplitude of response as a function of detuning frequency for Trapezoidal Hump

Figs. 4 to 6 show the responses of the system subjected to excitations from the three humps/bump obtained from the use of NDSolve within *Mathematica*^{TM} They show plots of amplitudes x(m) versus detuning frequency σ . In Fig.4 peak amplitude of 0.0135 m or 13.5 mm is observed for the circular hump. A jump phenomenonis also observed here. For the speed bump, a peak amplitude of 0.013 m or 13.0 mm is observed in Fig. 5. For the amplitude of response as a function of detuning frequency for the trapezoidal hump in Fig. 6, a peak amplitude of 0.0105 m or 10.5 mm and a jump phenomenon are observed. A percentage difference of 22.2% is observed between the peak amplitudes of the circular and the trapezoidal humps.

VI. CONCLUSION

A quarter-car model with passive elements was used in this research to investigate theoreticallythe car vibrations when crossing over circular humps, speed bumps and trapezoidal humps. Fixed hump/bump dimensions of 100 mm height and car velocity of 20km/h were considered. Ride comfort was considered through investigating the amplitude of vibration levels during crossing of the humps and bumps. The analysis of

the effects on the quarter-car model using the NDSolve within Mathematica™ showed that a nonlinear peak amplitude value of 13.5 mmwas obtained when crossing the circular hump. For the speed bump, a nonlinear peak amplitude of value of 13.0 mm was observed and a peak amplitude value of 10.5 mm was obtained for the trapezoidal hump. This means that a more destructive effect is expectedon either the vehicle or the passengers when crossing circular speed humps and a lesser effect when crossing trapezoidal speed humps. From the above results and analysis,it is observed that for most optimal result the best-suited calming hump is the trapezoidal design under which the system is exceptionally stable. Thus,this paper is recommending the trapezoidal speed hump as a more suitable calming device for adoption for Ghanaian roads.

REFERENCES

[1]. Arku. J., (2013). Daily Graphic News Paper, Ghana, August 13, 2013 Edition.
[2]. Akowuah, E., Ampofo, J. and Andoh, P.Y., (2015). Effect of speed ramps on pregnant women: A case study of travelers along Kumasi-Cape Coast highway, African Journal of Applied Research, Vol.2 (2), pp.19-30.
[3]. Emslie, I., (1997). Design and implementation of speed humps: Supplementary to national guidelines for traffic calming. Pretoria: Department of transport directorate.
[4]. Krylov, V. (2001). Generalization of ground elastic waves by road vehicles, Journal of Computational Acoustics, vol. 9 (3), pp. 919-933.
[5]. Dedovic, V. and Sekulic, D., (2012). Effect of shock vibrations due to speed control humps to the health of city bus passengers using Oscillation model with six DOF, International Conference on Traffic and Transport Engineering, Belgrade, November 29-30. Pp. 633-642.
[6]. Johnson, L. and Nedzesky, A. (2004). A comparative study of speed humps speed slots and speed cushions, ITE Annual Meeting.
[7]. Weber, T. (1998). Towards Canadian standard for the geometric design of speed humps, M. Engineering Thesis, Department of Civil and Environmental Engineering, Carleton University. Ottawa, Canada.
[8]. Berthod, C. (2011). Traffic calming, speed humps and speed cushions, 2011 Annual Conference of the Transportation Association of Canada, Edmonton, Canada.
[9]. Hassan, G.A. (2015). Car dynamics using quarter model and passive suspension, Part II: A novel simple harmonic hump, IOSR Journal of Mechanical and Civil Engineering (IOSR-JMCE) e-ISSN: 2278-1684, p-ISSN: 2320-334X, vol. 12(1) ver.II, pp. 93-100.
[10]. Garcia-Pozuelo, D., Gauchia, A., Olmeda, E. and Diaz, V. (2004). Bump modeling and vehicle dynamics prediction, Hindawi Publishing Corporation, Advances in Mechanical Engineering vol. 2014, Article ID 736576, 10 pages. http://dx.doi.org/10.1155/2014/736576.

LawrenceAtepor. "A Comparative Study of Nonlinear Dynamics of a Quarter-Car Model Excited by Three Types of Humps/Bumps used in Ghana." *American Journal of Engineering Research (AJER)*, vol. 9(8), 2020, pp. 186-193.